Nucleic Acids Research, 2025, **53**, gkae1184
https://doi.org/10.1093/nar/gkae1184
Advance access publication date: 9 December 2024
Molecular and Structural Biology

Isoleucine-to-valine substitutions support cellular physiology during isoleucine deprivation

Gautam Kok[1,†], Imre F. Schene[1,†], Eveline F. Ilcken[1,†], Paula Sobrevals Alcaraz[2], Marisa I. Mendes[3], Desiree E.C. Smith[3], Gajja Salomons[3], Sawsan Shehata[1], Judith J.M. Jans[4], Reza Maroofian[5], Tim A. Hoek[6], Robert M. van Es[2], Holger Rehmann[7], Edward E.S. Nieuwenhuis[1], Harmjan R. Vos[2] and Sabine A. Fuchs[1,*]

[1]Department of Metabolic Diseases, Wilhelmina Children's Hospital, University Medical Center Utrecht, Lundlaan 6, 3584 EA Utrecht, The Netherlands
[2]Center for Molecular Medicine, University Medical Center Utrecht, Oncode Institute, Heidelberglaan 100, 3584 CX Utrecht, The Netherlands
[3]Laboratory Genetic Metabolic Diseases, Amsterdam University Medical Centers, Meibergdreef 9, 1105 AZ Amsterdam, The Netherlands
[4]Laboratory of Metabolic Diseases, University Medical Center Utrecht, Lundlaan 6, 3584 EA Utrecht, The Netherlands
[5]Department of Neuromuscular Disorders, UCL Queen Square Institute of Neurology, Queen Square, London WC1N 3BG, United Kingdom
[6]Hubrecht Institute, Royal Netherlands Academy of Arts and Sciences, Uppsalalaan 8, 3584 CT Utrecht, The Netherlands
[7]Department Energy and Biotechnology, Flensburg University of Applied Sciences, Kanzleistraße 91–93 24943 Flensburg, Germany

*To whom correspondence should be addressed. Tel: +31 887553913; Email: s.fuchs@umcutrecht.nl
†The first three authors should be regarded as Joint First Authors.

Abstract

Aminoacyl-tRNA synthetases (ARSs) couple tRNAs with their corresponding amino acids. While ARSs can bind structurally similar amino acids, extreme specificity is ensured by subsequent editing activity. Yet, we found that upon isoleucine (I) restriction, healthy fibroblasts consistently incorporated valine (V) into proteins at isoleucine codons, resulting from misacylation of $tRNA^{Ile}$ with valine by wildtype IARS1. Using a dual-fluorescent reporter of translation, we found that valine supplementation could fully compensate for isoleucine depletion and restore translation to normal levels in healthy, but not IARS1 deficient cells. Similarly, the antiproliferative effects of isoleucine deprivation could be fully restored by valine supplementation in healthy, but not IARS1 deficient cells. This indicates I > V substitutions help prevent translational termination and maintain cellular function in human primary cells during isoleucine deprivation. We suggest that this is an example of a more general mechanism in mammalian cells to preserve translational speed at the cost of translational fidelity in response to (local) amino acid deficiencies.

Graphical abstract

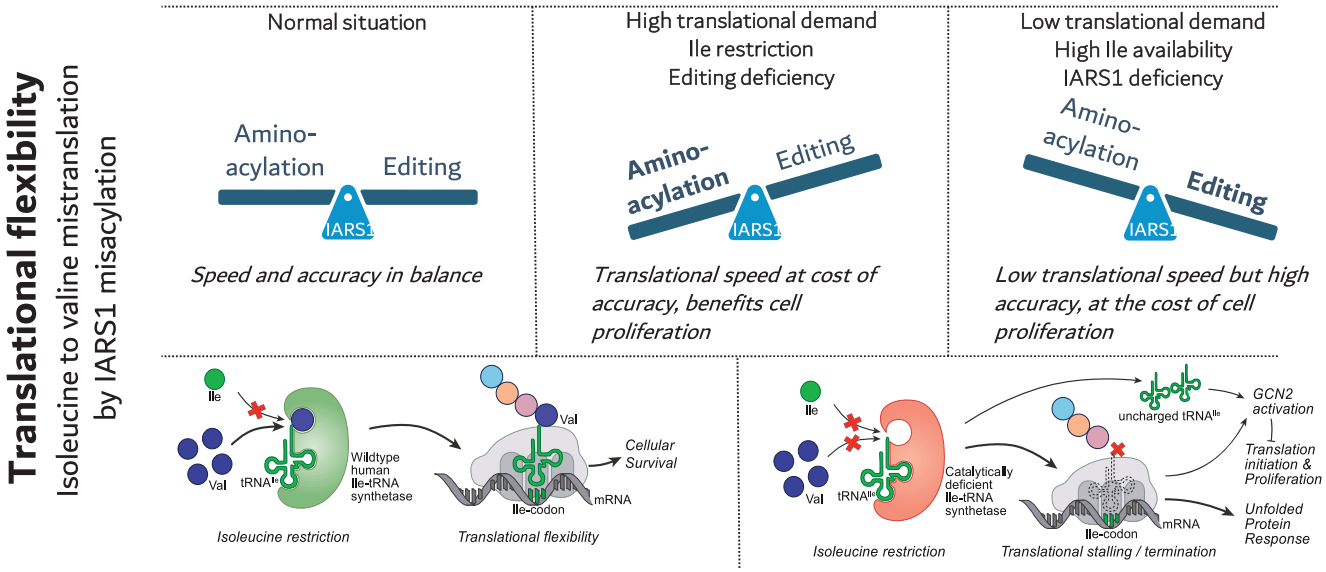

Received: September 15, 2022. **Revised:** November 8, 2024. **Editorial Decision:** November 11, 2024. **Accepted:** November 13, 2024

Introduction

Correct charging of tRNAs with their corresponding amino acid is crucial for accurately translating the genetic code into proteins. Central in this process are aminoacyl-tRNA synthetases (ARSs), enzymes that charge tRNAs with their corresponding amino acids. For each amino acid (a), a specific ARS (aARS) performs this role either in the cytosol (ARS1), in the mitochondria (ARS2) or both (KARS1, GARS1). Variants in ARS-genes are increasingly associated with human disease (1). Autosomal dominant variants in ARS-genes result in Charcot Marie Tooth polyneuropathies (2). The underlying mechanism was recently described for autosomal dominant GARS1 disease. By abnormal binding dynamics of GARS1 to Gly-tRNA^{Gly}, ribosome stalling occurs specifically in sensory neurons, leading to the GCN2-dependent stress response and peripheral neuropathy (3,4). Autosomal recessive variants in ARS-genes cause multi-organ disease (1). We previously hypothesized that symptoms arise in different organs due to insufficient canonical aminoacylation of tRNAs to meet translational demands, especially during times of high translation. This formed the basis for amino acid supplementation therapies for patients with ARS1 deficiencies, resulting in strikingly beneficial effects (5–7).

Nevertheless, the precise mechanism explaining how deficient aminoacylation of tRNAs leads to translational failure and organ-specific effects remains elusive. To address this, we analysed the molecular consequences of IARS1 deficiency in fibroblasts from two unrelated patients with the same compound heterozygous *IARS1* variants (NM_002161.5): c.1305G > C p. (Trp435Cys) and c.3377dup p. (Asn1126fs) (OMIM 600709) (1,5). Both variants are expected to affect the canonical aminoacylation function, with the Trp435Cys variant residing in the catalytic domain of IARS1, and the c.3377dup p. (Asn1126fs) variant likely leading to nonsense-mediated decay of the transcript (Supplementary Figure S1) (1,5). Accordingly, catalytic activity for these donors was severely decreased to 23% and 21% (5). We hypothesized that decreased catalytic activity would result in insufficient loaded tRNA^{Ile}, which may be compensated by misacylation. To our surprise, we consistently found that upon isoleucine restriction, healthy fibroblasts but not IARS1 deficient fibroblasts incorporated valine instead of isoleucine into proteins.

Sacrificing translational fidelity may represent a strategy to preserve protein synthesis during deprivation of specific essential amino acids, as is increasingly reported for unicellular organisms (bacteria and yeast) (8). It is known that ARSs can mis-activate tRNAs with structurally similar amino acids (9). Subsequent editing activity of various ARSs ensures extreme specificity under physiological conditions (10–12). To explore a putative rescue mechanism for unfavourable circumstances like (local) amino acid deficiencies induced by nutrition, physiological stress or disease states, we investigated the nature and consequences of misacylation by IARS1. We uncovered that IARS1 can indeed induce amino acid substitutions in healthy primary human cells. These substitutions were beneficial in preserving translation and promoting cell viability during nutritional stress. Not only does this contribute to further understanding of the consequences of IARS1 deficiency, but this may also represent a more general human strategy of ARSs to cope with unfavourable conditions.

Materials and methods

Ethical approval

Local medical ethical approval (Institutional Review Board of the University Medical Center Utrecht [STEM: 10-402/K, TC Bio 190489)] was obtained for use of the patient materials in this study. Written informed consent was obtained from all patients' parents.

Amino acid concentrations

Experimental amino concentrations were calculated as a percentage of average plasma concentrations of vegetarians (102 μM isoleucine; 210 μM leucine; 233 μM valine; 31 μM methionine; and 197 μM serine) (13). For most experiments, a 'normal medium' condition was used, which was based on Advanced DMEM/F12 (ADF12; ThermoFisher cat. 12634028), which contains ∼4× more isoleucine (416 μM) and ∼2× more valine (452 μM) than plasma. The complete formulation is available from the manufacturer.

Cell culture

Fibroblasts were obtained and cultured as described previously (5). Media with specific amino acid concentrations were based on amino-acid free DMEM/F12 (DF12; US Biological cat. D9811), supplemented with all amino acids (compared to ADF12), 1% GlutaMax, 1% penicillin/streptomycin (pen/strep) and 10% dialyzed foetal bovine serum (FBS; ThermoFisher cat. 26400044), or custom-made ADF12 (based on ThermoFisher cat. 12 634 010) without isoleucine/valine, supplemented with 1% GlutaMax, 1% pen/strep, 1% HEPES and 10% dialyzed FBS. HEK293T were cultured in DMEM (ThermoFisher cat. 10569010), supplemented with 1% pen/strep and 10% FBS. Cultures were tested for mycoplasma every 2 months.

Isolation of purified eGFP-tagged IARS1 protein

pJET_CMV_IARS1_[ED^{-}/Trp435Cys]_EGFP was transfected into 145 mm tissue culture dishes of HEK293T cells using PEI MAX (3:1 PEI:DNA) in 1.2 ml OptiMEM. After 48 h, cells were washed with phosphate-buffered saline (PBS), harvested by cell scraper and immediately sonicated in 200 μl PBS on ice at 87.5% amplitude for 10 s using 0.5 s cycles). Lysed samples were centrifuged at 17 000 × g for 10 min. Immunoprecipitation using GFP-Trap Agarose (Chromotek cat. GTA-20) was performed per manufacturer's protocol. Purified bead-protein complexes were supplemented with HALT protein inhibitor (ThermoFisher cat. #87786) in 15% glycerol and stored at −80°C until further use. Purity after elution was checked using mass spectrometry (Supplementary Figure S5). Protein concentration was measured using western blotting, using 1:5000 anti-GFP (Abcam, cat. AB290) by comparing against pure eGFP protein at 250 mg/ml).

tRNA$^{Ile[AAT]}$ production and purification

tRNA$^{Ile[AAT]}$ were produced from 1.81 μM top- and bottom oligos (5′-CCGCGTAATACGACTCACTATAGGCCGGTTAGCTCAGTTGGTtAGAGCGTGGTG and 5′-TmGGCCAGTACGGGGATCGAACCCGCGaCCTTGGCGTTATTAGCACCACGCTCTa) in 10× T4 ligase buffer (NEB, cat. B0202S) supplemented with 400 μM dNTPs (NEB, cat. N0447L) and 2325 units of DNA Polymerase I, Large (Klenow) Fragment

(NEB, cat. M0210S) and incubated at 25°C for 15 min. Fragments were isolated from a 2% Agarose in TBE gel purified using a PureLink PCR purification kit (ThermoFisher, cat. K310001). Fragments were *in vitro* transcribed using 1 mg DNA, NTP reaction buffer, 5 mM DTT and 100 units T7 RNA polymerase (NEB, cat. E0204S) at 37°C for 5 h. The reaction was stopped by DNase treatment at 37°C for 15 min. Reaction volume was adjusted to 180 µl with water and 1:10th vol. of 5 M ammonium acetate was added. tRNA was purified by three sequential isolation steps with 1:1 phenol/chloroform and precipitated using 2 × 100% ethanol for 30 min at −20°C. tRNA was collected by centrifugation, rinsed with cold 70% ethanol, resuspended in water and stored at −80°C for use in aminoacylation experiments.

Aminoacylation activity

IARS1 activity was measured in fibroblast lysates as described previously, with four technical replicates per condition and donor (5). In addition, IARS1 was assessed in purified proteins. Ten microlitre of pure protein were incubated in triplicate at 37°C for 10 min in a reaction buffer containing 50 mmol/l Tris buffer, pH 7.5, 12 mmol/l $MgCl_2$, 25 mmol/l KCl, 1 mg/ml bovine serum albumin, 0.5 mmol/l spermine, 1 mmol/l ATP, 0.2 mmol/l *Escherichia coli* total tRNA or 25 µg synthesized $tRNA^{Ile[AAT]}$, and 1 mM or 600 µM of [$^{13}C_6$, ^{15}N]-isoleucine and/or [^{15}N]-valine. The reaction was terminated using trichloroacetic acid. After sample washing with trichloroacetic acid, ammonia was added to release the labelled amino acids from the tRNAs. [D_3]-leucine and [^{13}C]-valine were added as internal standards and the labelled amino acids were quantified by LC-MS/MS.

Lentivirus production

Lentiviruses were produced in HEK293T cells (15 cm dish). At 80% confluency, they were transfected with 10 µg GFP-α-catenin lentiviral plasmid DNA, 6.6 µg psPAX2 (Addgene #12260), 3.3 µg pMD2.G (Addgene #12259) and PEI MAX (3:1 PEI:DNA), in 1 ml OptiMEM. Both psPAX2 and PMD2.G were a gift from Trono *et al*. Media were refreshed after 24 h. Then, media containing the virus was collected after 48 and 72 h. Virus was concentrated using Lenti-X concentrator (Takara, cat. 631231), resuspended in 2 ml DMEM and stored at 4°C for short-term use, and at −80°C for long-term use.

Lentiviral transduction

Fibroblasts were harvested by trypsinization, washed and resuspended in culture medium with 12 µg/ml polybrene, then mixed 1:1 with concentrated virus and incubated for 1 h at 37°C. Cells were plated on a 6-well plate with 6 µg/ml polybrene and incubated for 24 h. Culture media were refreshed and cells were allowed to grow to 70% confluency. Transduced cells were selected by fluorescence-activated cell sorting (FACS).

Amino acid substitution sample preparation

Stable GFP-α-catenin-expressing fibroblasts were created by lentiviral transduction. GFP^+ cells were selected by FACS and cultured to 6 × 15 cm dishes per condition. At 70% confluency, cells were washed once with PBS, then incubated for 72 h with the desired concentrations of isoleucine and valine. After washing with ice-cold PBS, cells were harvested with a cell scraper and pooled per condition. Pooled samples were washed twice with PBS and immediately lysed in RIPA buffer (ThermoFisher cat. 89900) with 1% Halt (ThermoFisher cat. 87786) for 30 min. Immunoprecipitation using GFP-Trap Agarose (Chromotek cat. GTA-20) was performed per manufacturer's protocol. Cells were additionally washed three times in ice-cold PBS, and transferred to new Eppendorf tubes before the final wash. Samples were stored at −80°C before mass spectrometry.

Mass spectrometry

After immuno-precipitation of GFP-α-Catenin, proteins were denatured in 8 M urea, 1 M ammonium bicarbonate (ABC) containing 10 mM tris (2-carboxyethyl) phosphine hydrochloride to reduce and 40 mM 2-chloro-acetamide to alkylate the cysteines. After 4-fold further dilution with 1 M ABC and digestion with trypsin (250 ng/200 µl), peptides were separated from the sepharose beads and desalted with homemade C-18 stage tips (Affinisep, Le Houlme, France). Peptides were separated on a 25 cm column (75 µm ID fused silica capillary with emitter tip, made in house) packed with 1.9 µm aquapur gold C-18 material (Dr Maisch, Ammerbuch-Entringen, Germany) using a 2 h gradient (0–80% acetonitrile), delivered by an easy 1200 nano HPLC (Thermo Scientific, Waltham, MA). Peptides were electrosprayed directly into a Fusion Tribrid-Orbitrap (Thermo Scientific) and analysed in data-dependent mode with the resolution of the full scan set at 240 000, after which the top N peaks were selected for higher energy collision-induced dissociation fragmentation (set at a normalized energy of 30%) and detection in the Iontrap with a target setting of 5000 ions. Raw files were analysed with Proteome Discoverer (PD) software (Thermo, versions 2.4.0.305 & 2.5.0.400). For identification, a fasta file of the *Homo sapiens* protein Catenin alpha-1 (CTNA1, UniProt P35221) was used to perform a search with the standard Consensus Workflow for Label free quantification of the precursor peptide and the standard Processing Workflow for Orbitrap, Sequest and Percolator, with carbamido-methylation of cysteine set as fixed modification. The required substitutions from Isoleucine (Ile) to other amino acids were set as a variable modification in consecutive analysis runs. The mass accuracy of the recalibration node was set to 20 ppm for the precursor and the fragmentation to 0.5 Da. The main search settings were 5 ppm for the precursor and 0.5 Da for the fragments. The traces of the peptides chromatograms were extracted from the result files of PD and plotted using R (version 4.0.4) through RStudio (version 1.5.64). The mass spectrometry proteomics data have been deposited to the ProteomeXchange Consortium via the PRIDE partner repository (http://www.ebi.ac.uk/pride with the dataset identifier PXD033426). Mass spectrometry on immunoprecipitated IARS1-eGFP was done essentially the same as described above. However, raw files were searched on 3 January 2022 with the standard settings of MaxQuant (version 2.4.9.0) against the Human database (UniProt; Taxon ID 9606), with the intensity based absolute quantification option included.

Cloning of wildtype, catalytic domain deficient and editing-domain deficient eGFP-tagged IARS1

Wildtype IARS1 was isolated from TriZOL-isolated RNA from wildtype fibroblasts using reverse transcriptase and cloned into a general lentiviral backbone with a CMV promoter to create pLV_CMV_IARS1. The editing domain of

IARS1 resides from amino acid 199–397 and is highly conserved. An editing-domain deficient (ED$^-$) variant was created by substitution of the fully conserved amino acids 224–233 with an alanine decapeptide using In-Fusion HD cloning (Takara cat. 639648) (14). Additionally, a variant containing the catalytic domain patient mutation Trp435Cys was created following the same method. CMV_IARS1, CMV_IARS1_ED$^-$, CMV_IARS1_Trp435Cys and eGFP (from pEGFP-C3) were amplified using PCR and cloned into a pJET1.2 backbone (ThermoFisher cat. K1231) using In-Fusion HD cloning with the addition of a linker peptide (5′-TCCGGACTCAGATCT CGAGCTCAAGCTTCGAATTCTGCAGTCGACGCCACC ; N-SGLRSRAQASNSAVDAT; Integrated DNA technologies) to form pJET_CMV_IARS1_[ED$^-$/Trp435Cys]_EGFP. These plasmids can be obtained through Addgene (#212322 and #212323).

Cloning of dual-fluorescent translation reporter

Three custom dual-fluorescent reporters of translation termination were adapted from pmGFP-P2A-K0-P2A-RFP (Addgene #105686) and pmGFP-P2A-K20 (AAA)-P2A-RFP (Addgene #105688), which were gifted by Juszkiewicz *et al.* (15). The CMV-GFP-P2A-K0/K20 (AAA)-P2A-RFP cassettes were amplified by PCR and subcloned into a pJET1.2 backbone vector. To create the CMV-GFP-P2A-15xIle-P2A-RFP reporter, a geneblock containing 15× isoleucine codons was ordered (Integrated DNA technologies) and cloned in-frame in-between the P2A sites using In-Fusion HD cloning. These plasmids can be obtained through Addgene (#185618, #185619 and #185620).

Dual-fluorescent reporter of translation

A 6-well of fibroblasts per condition was washed with PBS, and media were replaced to culture media with normal concentrations of isoleucine and valine, isoleucine depletion (0%) or isoleucine depletion with valine depletion or supplementation (1% or 10× of plasma). Cells were immediately transfected with pJET-CMV-GFP-[empty/15xIle/20xLys$_{AAA}$]-mCherry using Lipofectamine 3000 according to manufacturer's protocol, except replacing OptiMEM by isoleucine- and valine-free custom-made ADF12 without supplements. After 24 h, cells were washed once with PBS, harvested by trypsinization and kept on ice onwards. Cells were resuspended in ice-cold FACS buffer (PBS with 2 mM ethylenediaminetetraacetic acid and 0.5% bovine serum albumin) with 1× DAPI and transferred to filter-capped FACS tubes. Fluorescence was measured on a CytoFLEX S (Beckman Coulter) flowcytometer (405→450 ± 45 nm, 488→525 ± 40 nm, 561→610 ± 20 nm). Gating and calculations were performed in FlowJo V10.8 (BD Biosciences). The gating strategy is attached in Supplementary Figure S7. In summary, from single cells selected by FSC/SSC, live cells (DAPI$^-$) were selected. From the GFP$^+$ cells, the median ratio between the red- and green fluorescence was calculated, and each condition was normalized to the normal isoleucine value. Statistical analyses and data visualization were performed in GraphPad Prism 9.

Proliferation assay

Fibroblasts were seeded in quadruplicate on E-Plate 96 PET (Agilent, cat. 300600910) at 3500 cells/well in normal culture medium. After 24 h, wells were washed twice with PBS, and medium with the desired amino acid concentrations was applied. Proliferation of fibroblasts was evaluated by continuous impedance analysis over 2 or 5 days using a real-time cell analyser (xCELLigence MP, ACEA Biosciences). Per donor, impedance was normalized against the 100% amino acid concentration condition.

Intracellular amino acid concentrations

Fibroblasts of three healthy donors, of both patients and of a third patient homozygous for catalytic variant c.243A > C p.(Arg81Ser) were seeded on 6-well plates to contain ∼50.000 cells/well at time of harvest in normal culture medium. After 24 h, wells were washed twice with PBS, and medium with the desired amino acid concentrations was applied. After another 24 h, wells were washed twice with PBS and three were immediately lysed in RIPA buffer (ThermoFisher cat. 89 900) with 1% Halt (ThermoFisher cat. 87786) for 30 min. Three wells were harvested in 80% methanol by cell scraping, vortexed rigorously and centrifuged (5 min at 16 600 × g) at 4°C. Supernatant was stored at −80°C for determining intracellular amino acid concentrations using mass spectrometry as reported previously (16). Data were corrected for the difference between the median ratio between culture media or plasma and intracellular amino acid concentrations from Baydoun *et al.*, (17) Dall'Asta *et al.* (18) and Bergström *et al.* (19), and the ratio in our own analysis (Figure 3A; Supplementary Table S2). This correction was required because no reliable cell volumes were available. For the same reason, concentrations of individual amino acids were normalized to the average concentration of all amino acids per condition, i.e. for each donor and medium condition.

Prediction of functional effects of amino acid substitutions

Lists of various amino acid residues in human transcripts were prepared using the 'whole human exome sequence space' database. The effects of various amino acid substitutions on protein structure and function were predicted using Polymorphism Phenotyping v2 (PolyPhen-2) in batch mode and HumVar classifier model (20). Data were further processed, analysed and visualized using R (v4.2.1).

RNA sequencing and analysis

A 6-well of fibroblasts per condition was washed with PBS, and media were replaced to culture media with normal concentrations of isoleucine or isoleucine depletion (1% of plasma). After 72 h, before confluency was reached in any condition, total RNA was isolated using Trizol LS reagent (Invitrogen) and stored at –80°C until further processing. mRNA was isolated using Poly (A) Beads (NEXTflex). Sequencing libraries were prepared using the Rapid Directional RNA-Seq Kit (NEXTflex) and sequenced on a NextSeq500 (Illumina) to produce 75 base long reads (Utrecht DNA Sequencing Facility). Sequencing reads were mapped against the reference genome [genome sequence release 33 (GRCh38.p13)] using BWA41 package (mem –t 7 –c 100 –M –R). Normalized counts were obtained by applying the DESeq2 variance-stabilizing transformation to the read counts using the 'DESeq2' R package (21). Principal component analysis was performed with the 5000 most variable genes and plotted using the DESeq2 'plotPCA' function. Differentially expressed genes between normal and 1% isoleucine conditions were cal-

culated using Deseq2, correcting for Control/Patient-batch effects [design = ~type ('control' or 'IARS1') + isoleucine ('1%' or '100%')], using thresholds of 'padj' < 0.05 and 'log2FoldChange' > 1. Finally, genes that were upregulated in IARS1 patient versus control lines, which were also upregulated upon isoleucine depletion, were extracted using a threshold of 0.5-fold (log2) increase between the average of groups. Similarly, genes that were downregulated in IARS1 patient and downregulated upon isoleucine depletion, were extracted using a threshold of 0.5-fold (log2) decrease between the average of groups. Heatmaps were created using Microsoft Excel. Gene set enrichment analysis of genes that were up/down regulated upon isoleucine depletion, and in IARS1 patient versus control lines, was performed using Enrichr (22). RNA sequencing results are available in Supplementary Table S1.

Results

IARS1 generates I > V substitutions in human fibroblasts upon isoleucine deprivation

To investigate if isoleucine deprivation causes amino acid substitutions, we created primary fibroblast lines derived from healthy donors that stably express a fusion protein of green fluorescent protein (GFP) and alpha catenin (CTNA1). We immunoprecipitated the fusion protein from protein lysates and performed mass spectrometry analysis to search for isoleucine substitutions in stable CTNA1 peptides containing a single isoleucine residue (TSVQTEDDQLIAGQSAR and NAGNEQDLGIQYK) (Figure 1A). We did not observe any I > V substitutions in fibroblasts cultured under normal conditions. However, upon isoleucine depletion (1% of normal plasma concentrations), we found a strong increase of I > V substitutions in both peptides, which did not further increase upon additional valine supplementation (Figure 1B, Supplementary Figure S2B). Isoleucine deprivation did not introduce I > V substitutions in fibroblasts from patients with impaired catalytic IARS1 activity while supplementation of additional valine led to minimal I > V substitutions (Figure 1B). This suggests that misacylation of $tRNA^{Ile}$ by wildtype IARS1 is responsible for the observed I > V substitutions. Additionally, we found I > M substitutions upon isoleucine depletion in both healthy control- and patient-derived cells (Supplementary Figure S2A and B), without beneficial effects on cell proliferation upon methionine supplementation (Supplementary Figure S4). Isoleucine (AUU, AUC and AUA) and methionine (AUG) codons only differ at the third codon wobble position (8). Methionine incorporation may thus result from ribosomal mispairing, possibly mediated by post-transcriptional modifications at the wobble of the anticodon of $tRNA^{Ile}$. We could not reliably identify any other I > X substitutions upon thorough screening of the mass-spectrometric data.

(Mis)acylation activity of IARS1 may overwhelm editing activity

To understand why IARS1 would tolerate misacylation, we set out to investigate *in vitro* isoleucine and valine aminoacylation by wildtype IARS1 and IARS1 with deficient catalytic or editing function. However, the diagnostic aminoacylation assay measures intracellular tRNA-loading and not individual ARS activity. To determine IARS1 activity in isolation, we isolated IARS1 by eGFP-tagging and immunoprecipitation. Mass spectrometry analysis of our IARS1-eGFP isolates revealed minimal co-precipitation of only multisynthetase complex partner proteins (Supplementary Figure S5). Using the isolated IARS1, we confirmed significant *in vitro* misacylation of total tRNA with valine by IARS1 (in the absence of VARS1), which was strongly decreased (76%) in catalytically deficient (Trp435Cys) IARS1 (Figure 2A, $P < 0.01$), putatively because the intact editing activity outbalances the deficient catalytic activity. We found similar results using *in vitro* transcribed $tRNA^{Ile}$, ruling out any possible misacylation of $tRNA^{Val}$ (Figure 2B) and found increased misacylation with increasing valine over isoleucine concentrations, putatively because in wildtype IARS1, the catalytic activity increasingly outbalances the editing activity with increasing valine over isoleucine availability (Figure 2C). Note that the 2 mM valine condition is comparable to the 10× valine relative to plasma (2330 μM) condition in other experiments. To confirm this interplay between catalytic and editing activity as the mechanism underlying mistranslation, we created an editing domain deficient variant of IARS1 by replacing part of the highly conserved editing domain by an alanine decapeptide, as was done previously for the bacterial variant of the protein (14). Unfortunately, the resulting protein was unstable as shown by low levels of green fluorescence and very low protein yields (Supplementary Figure S5), precluding accurate aminoacylation activity measurements.

Intracellular amino acid concentrations in IARS1 deficiency

To understand these amino acid medium concentration-dependent effects and relate them to intracellular concentrations, we measured amino acid concentrations in the different deprivation media conditions in fibroblasts derived from healthy controls and IARS1 deficient patients. In general, intracellular concentrations are higher than plasma concentrations, putatively due to active import of cells. The human *in vivo* intracellular to plasma ratio of isoleucine and valine was previously determined at 1.75 ± 0.79 and 1.16 ± 0.42, respectively (19). Both the *in vivo* intracellular and plasma concentrations of valine were at least double that of isoleucine (13,19). Normalized intracellular concentrations of amino acids (Figure 3A and B) were generally comparable in IARS1 patient fibroblasts and healthy fibroblasts. Upon isoleucine restriction (1%, 1.02 μM), intracellular amino acid concentrations were non-significantly increased in IARS1 patient fibroblasts compared to healthy fibroblasts, except for aspartic acid (Asp), which was significantly lower ($P < 0.01$; Figure 3C). With supplementation of valine to 2330 μM (10× plasma, ~5.2× increase from culture media at 452 μM), intracellular valine concentrations increased linearly (healthy: 5.0×, IARS patient: 4.7×; Figure 3B) and concentrations were significantly higher in patient-derived fibroblasts compared to healthy controls, putatively due to upregulated active amino acid import (Figure 5B and C).

I > V substitutions support translation and proliferation in human fibroblasts

To test whether isoleucine-deprived cells benefit from a certain rate of I > V substitution to maintain translation of isoleucine-rich regions, we adapted a dual-fluorescent reporter (15) to contain a cassette of eGFP and mCherry, interceded by an isoleucine-rich region (Figure 4A). Regular translation of this

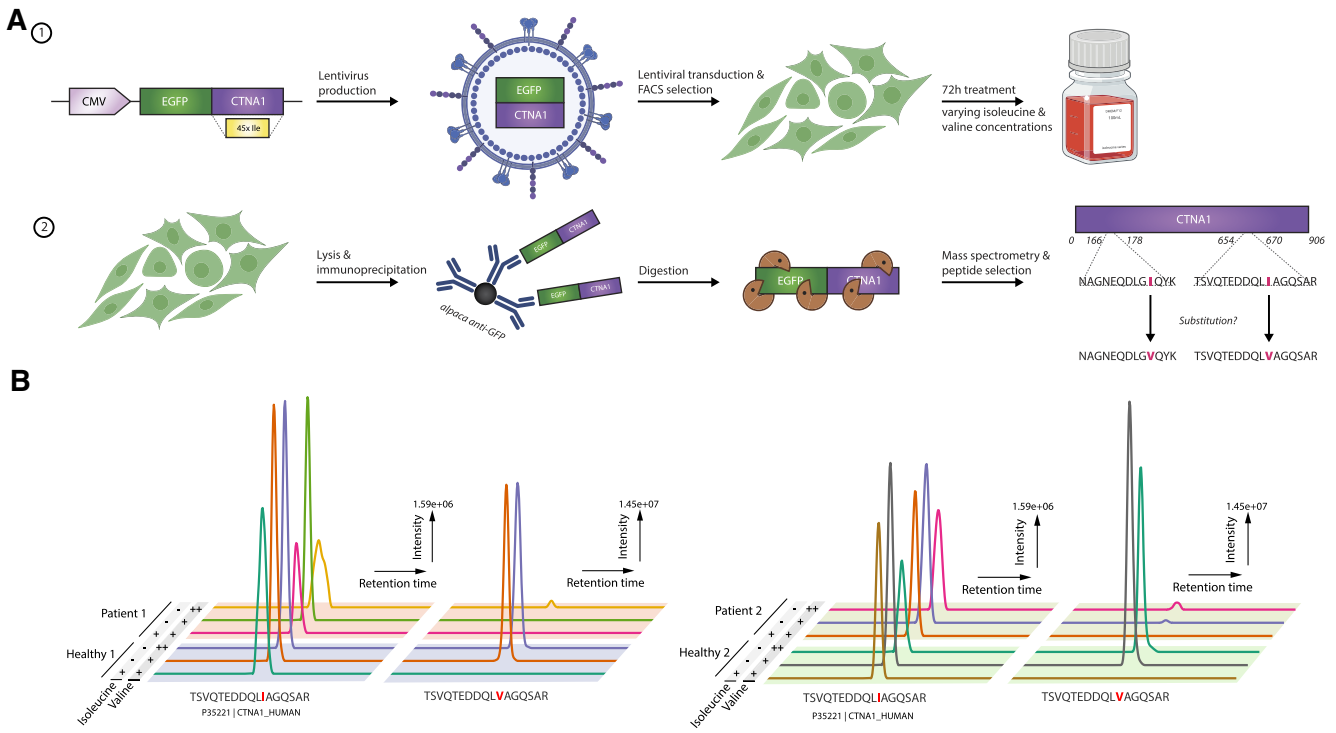

Figure 1. Detection of I > V substitutions upon isoleucine restriction. (**A**) Schematic representation of sample preparation for mass spectrometry to identify amino acid substitutions in peptides of the exogenously expressed GFP-Catenin Alpha 1 protein (CTNA1). See methods for amino acid concentrations. (**B**) Extracted ion chromatograms of peptides containing a single isoleucine or isoleucine > valine substitution in healthy fibroblasts or fibroblasts from patients with IARS1 deficiency. Amino acid concentrations are as follows: isoleucine: + = normal media with 416 μM, − = 1% plasma at 1.02 μM; valine: + = normal media with 452 μM, ++ = 10× plasma at 2330 μM.

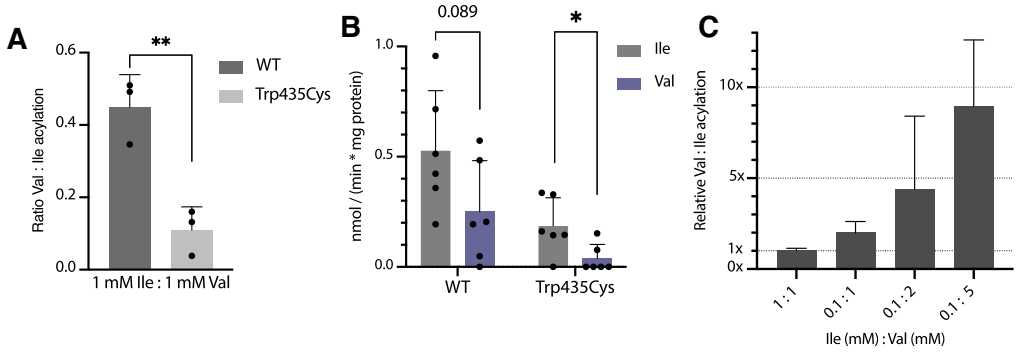

Figure 2. (Mis)acylation activity of IARS1 may overwhelm editing activity. (**A**) *In vitro* aminoacylation activity of purified wildtype and Trp435Cys mutant IARS1-eGFP for isoleucine and valine at 1 mM using *E. coli* bulk tRNA. (**B**) *In vitro* aminoacylation activity of purified wildtype and Trp435Cys mutant IARS1-eGFP for isoleucine and valine at 600 μM using *in vitro* transcribed $tRNA^{Ile\text{-}AAT}$. Six replicates per condition, measurements resulting in 'negative' activity after blank subtraction were set to zero. (**C**) *In vitro* aminoacylation activity of purified wildtype IARS1-eGFP for isoleucine and valine at different concentrations using *E. coli* bulk tRNA. Note that the 2 mM valine condition is comparable to the 10× valine condition in other experiments (2330 μM). Two-sided unpaired Student's *t*-test with equal variance: $^{**}P < 0.01$; each bar represents the mean of three to six technical replicates ± SD. Large variations in measurements stem from the difficulty of using consistent protein amounts per assay, likely due to protein attachment to beads.

cassette results in equal amounts of GFP and Cherry fluorescence while translational termination in the interceding region decreases Cherry to GFP ratios (Supplementary Figure S3A and B). We transfected the reporter into four healthy donor fibroblast lines and the two fibroblast lines from patients with IARS1 deficiency, incubated the cells for 24 h in various medium conditions, and analysed translational function by flow cytometry. As expected, isoleucine deprivation impaired translation of the isoleucine-rich region, and this effect was stronger in IARS1 patient fibroblasts than in healthy fibroblasts (Figure 4B). Supplementation of additional valine restored translation to normal levels in healthy cells but only marginally in IARS1 deficient cells (Figure 4B, Supplementary Figure S3C). This indicates that I > V substitutions help to prevent translational termination during isoleucine deprivation and that this mechanism depends on IARS1 catalytic activity.

To determine the effect of I > V substitutions on cellular functions, we quantified proliferation of human fibroblasts cultured under various medium conditions. In healthy fibroblasts, proliferation decreased upon isoleucine depriva-

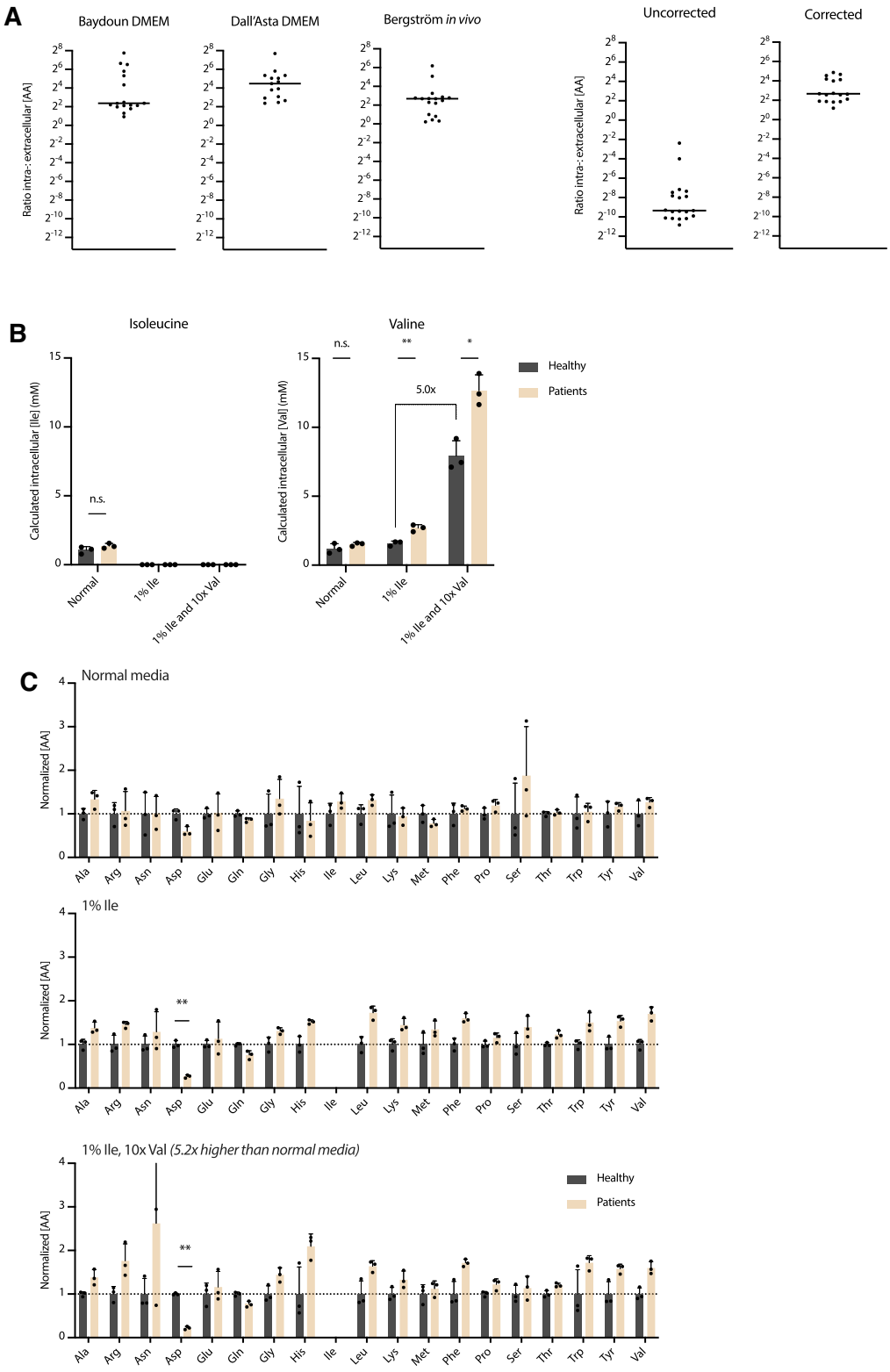

Figure 3. Intracellular amino acid concentrations. (**A**) Ratio of intra- and extracellular amino acid concentrations from Baydoun *et al.*, (17) Dall'Asta *et al.*, (18) and Bergström *et al.* (19). Each dot represents an amino acid. The corrected data reflects our measurements with a factor for the difference between the median ratio in literature and the ratio in our analysis. This correction is required because we have no reliable data on the actual cell volumes. (**B** and **C**) Intracellular concentrations (mM) of isoleucine and valine in healthy ($n = 3$) and IARS1 patient ($n = 3$) fibroblasts cultured with varying concentrations of isoleucine and valine, calculated by factor and normalized to the total concentration of all amino acids for that sample within each condition. This method assumes equal total amino acids in each sample. Two-sided unpaired Student's *t*-test with equal variance, with Bonferroni correction for multiple testing: n.s. $P \geq 0.05$, $*P < 0.05$, $**P < 0.01$; each dot represents the average of three technical replicates; bars depict mean ± SD.

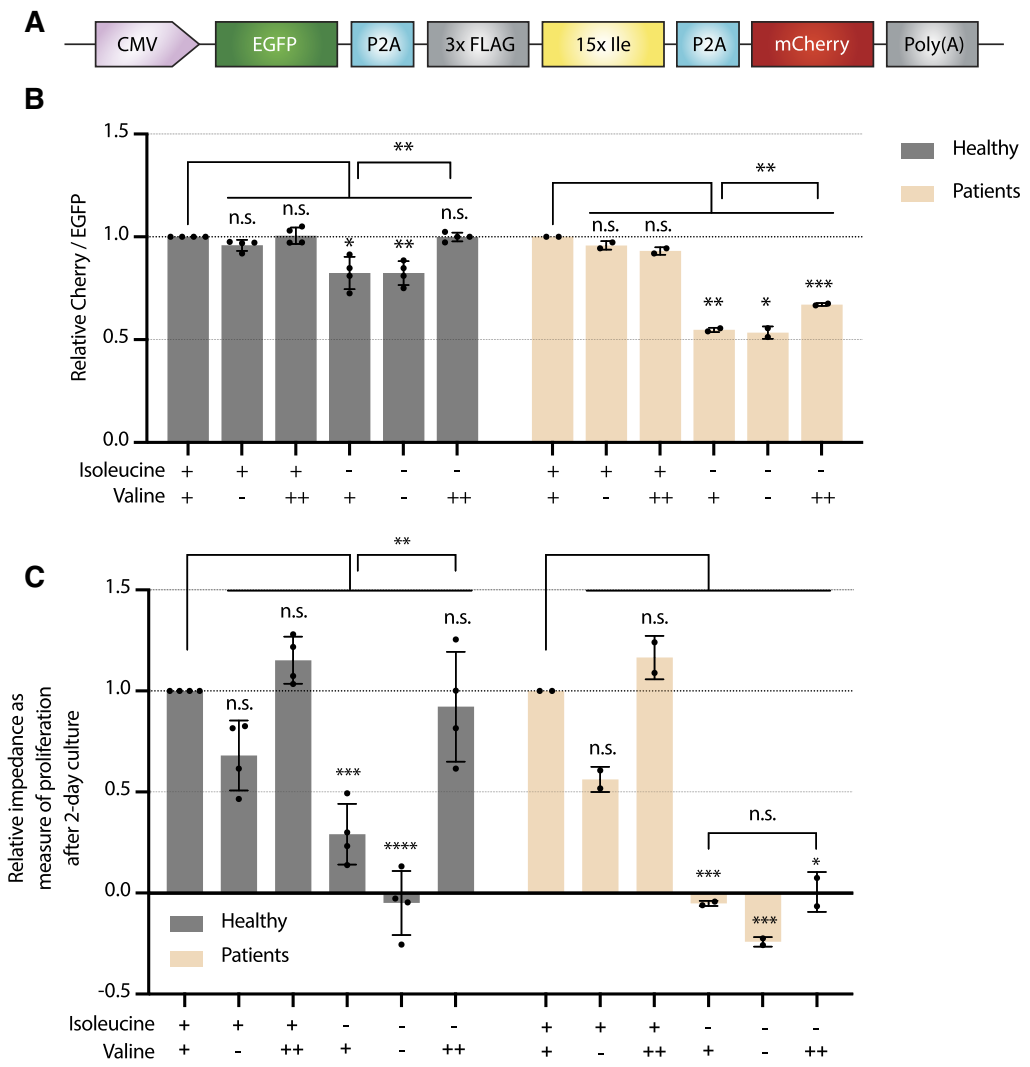

Figure 4. I > V substitutions prevent translational termination and maintain cellular growth. (**A**) Design of the ribosomal stalling reporter plasmid. (**B**) Relative fluorescence of Cherry/GFP in healthy and IARS1 deficient patient-derived fibroblasts under varying concentrations of isoleucine and valine (isoleucine: + = 100%, − = 0% | valine: + = 100%, − = 1%, ++ = 10× plasma); two-sided unpaired Student's *t*-test with equal variance, with Bonferroni correction for multiple testing: n.s. $P \geq 0.05$, *$P < 0.05$, **$P < 0.01$, ***$P < 0.001$. (**C**) Normalized impedance as a measure of proliferation as measured with the xCELLigence MP real-time-cell-analyzer after 2-day culture in varying concentrations of isoleucine and valine (isoleucine: + = 100%, − = 1% | valine: + = 100%, − = 1%, ++ = 10× of plasma concentrations); negative values represent cell death; two-sided unpaired Student's *t*-test with equal variance, with Bonferroni correction for multiple testing: n.s. $P \geq 0.05$, *$P < 0.05$, **$P < 0.01$, ***$P < 0.001$, ****$P < 0.0001$; each dot represents the average of four technical replicates; bars depict mean ± SD.

tion (1% of plasma concentrations) and decreased further upon additional valine deprivation (1% isoleucine and 1% valine, $P = 0.021$) (Figure 4C). In comparison, fibroblasts from patients with IARS1 deficiency were more severely affected by isolated isoleucine deprivation ($P = 0.039$) but not by isolated valine deprivation ($P = 0.422$). Strikingly, additional valine supplementation (10× plasma concentration) could rescue the antiproliferative effects of isoleucine deprivation almost completely in healthy cells ($P = 0.007$), while additional leucine, methionine or serine could not (Figure 4C, Supplementary Figure S4). In IARS1 deficient cells, additional valine supplementation did not rescue the antiproliferative effects of isoleucine deprivation ($P = 0.511$) (Figure 4C). Together, these findings indicate that I > V substitutions, originating from misacylation of $tRNA^{Ile}$ with valine by catalytically active IARS1 help to preserve cellular functions and viability during isoleucine deprivation.

Translation termination and unfolded protein response aggravated by IARS1 deficiency

As observed with the dual fluorescent reporter, isoleucine deprivation led to translation termination in fibroblasts and this effect was more pronounced and could not be rescued by valine in fibroblasts from patients with IARS1 deficiency. Principal component analysis of RNA sequencing data of these fibroblasts discriminated two clusters based on isoleucine concentrations rather than on healthy versus patient status (Figure 5A). Genes that were upregulated upon isoleucine deprivation were associated with mTORC1, amino acid transport, the unfolded protein response, NF-κB signalling, and apop-

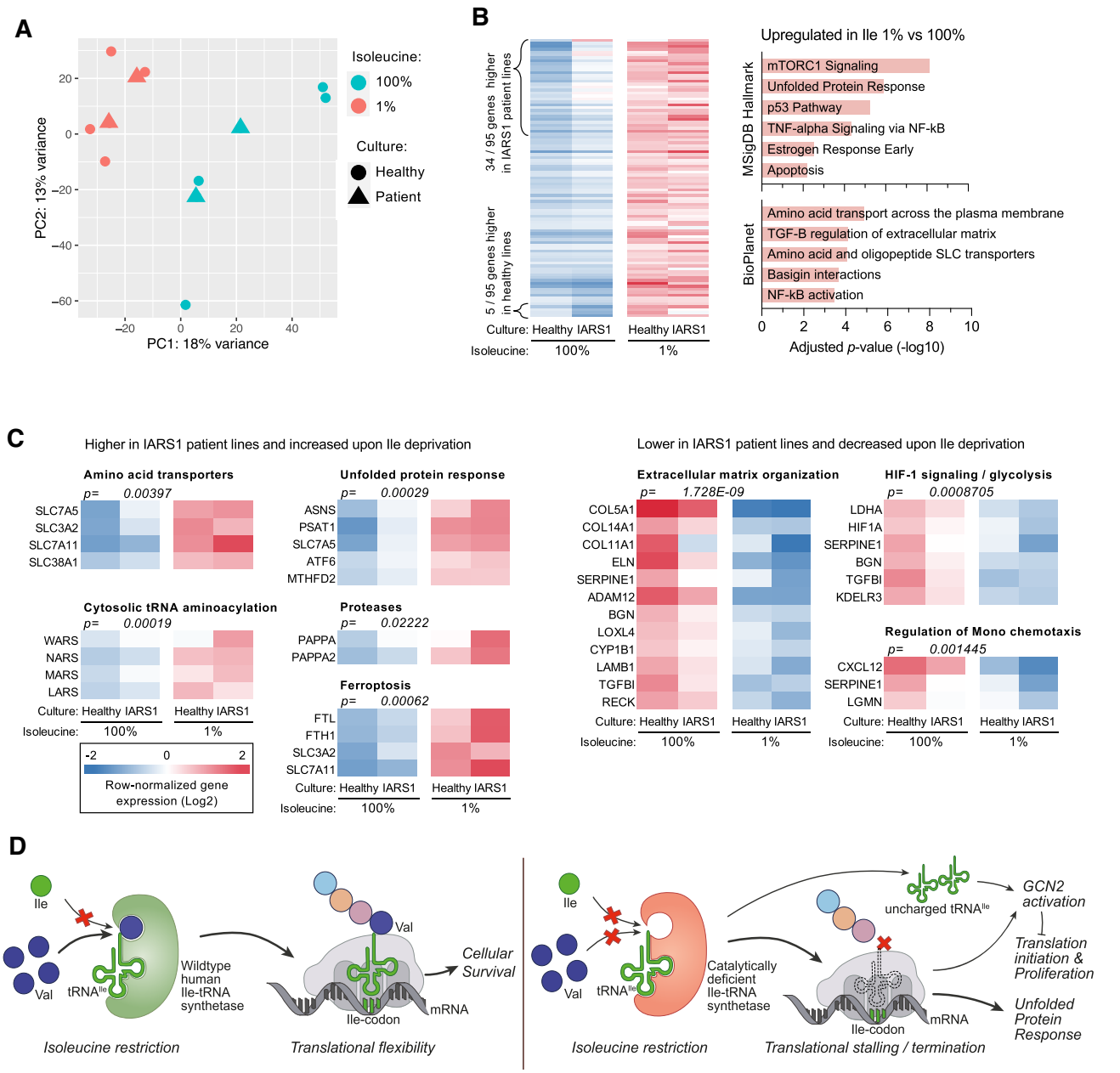

Figure 5. Reaction to isoleucine deprivation is aggravated by IARS1 deficiency. (**A**) Principal component plot of fibroblasts from healthy persons and patients with IARS1 deficiency cultured in normal (100%) and isoleucine deprived medium (1% of normal plasma concentrations). (**B**) Genes with increased expression in fibroblasts cultured in 1% versus 100% isoleucine concentrations and corresponding pathways; fold changes are provided in Supplementary Table S1C. (**C**) Differentially expressed genes between fibroblasts from healthy controls and patients with IARS1 deficiency, which further deviate with isoleucine deprivation. (**D**) Proposed IARS1 function and disease mechanism in IARS1 deficiency in response to isoleucine deprivation. Wildtype (catalytically active) IARS1 attaches the structurally similar valine instead of isoleucine to $tRNA^{Ile}$ upon (local) isoleucine restriction. I > V substitutions in proteins are generally benign and thus support translation and cellular function. Catalytically deficient IARS1 cannot attach valine instead of isoleucine, putatively leading to an increase of uncharged $tRNA^{Ile}$ and activation of GCN2, thereby inhibiting translation initiation and proliferation. Termination of translation further activates the unfolded protein response and apoptosis.

tosis and were generally expressed higher in IARS1 deficient than healthy fibroblasts (Figure 5B). Reasoning that IARS1 deficiency may induce an exaggerated physiological response to isoleucine deprivation, we found IARS1 specific upregulation of amino acid transporters, cytosolic tRNA amino acid synthetases, the unfolded protein response, proteases and ferroptosis, while pathways associated with proliferation (glycolysis, extracellular matrix organization) were downregulated (Figure 5C). Together, these results support a disease mechanism of insufficient $tRNA^{Ile}$ aminoacylation to meet translational demands, resulting in translation termination at isoleucine codons, leading to an increase in (poly)peptides terminated prior to isoleucine incorporation and increased unfolded protein response, cellular stress, and apoptosis. In case of isoleucine deprivation, this reaction is more pronounced in IARS1 deficiency because of an additional failure to compensate with misacylation of $tRNA^{Ile}$ with valine (Figure 5D).

Discussion

In this study, we show that healthy human primary cells deprived of isoleucine substitute isoleucine for valine and thereby maintain translation and proliferation. Using cells derived from patients with catalytically deficient IARS1, we were able to attribute the observed isoleucine-to-valine substitutions to IARS1 misacylation of $tRNA^{Ile}$ with valine and not to alternative ribosomal decoding.

Accurate protein translation (1:3 300) is believed to be essential to life (11). Indeed, IleS from *E. coli* evolved an editing domain to hydrolyse non-cognate amino acids such as valine that are frequently mis-activated by the catalytic domain (1:180) (23). This mechanism ensures low error rates (1:50 000) under normal conditions (11). Very recently, it was discovered that this IleS editing domain does not display higher hydrolysis rates of amino acids that are often mis-activated compared to amino acids that are rarely mis-activated (24). This suggests that IARS1 evolved to prevent hydrolysis of correctly activated Ile-$tRNA^{Ile}$ and not to minimize misacylation of $tRNA^{Ile}$, thus supporting translational speed at the expense of translational fidelity. This is in line with our finding that human IARS1, in which the editing domains of *E. coli* IleS are highly conserved (52% positives, 31% exact match), can activate valine and subsequently misacylate $tRNA^{Ile}$ with valine, especially during isoleucine deprivation, and that misacylation is largely prevented by patient mutations that lead to impaired catalytic but conserved editing activity of IARS1 (Figure 4A). Our results suggest that while ARS catalytic and editing function is balanced under normal conditions, the editing function can be outbalanced by increased alternative over cognate amino acids ratios and the catalytic function can be outbalanced by inactivating mutations.

Recently, a similar mechanism of WARS1-induced W > F substitutions was discovered in both cancer cells (25). WARS1 is different from IARS1 by the absence of an editing function, yet these W > F substitutions preserved translation but generated dysfunctional proteins that were expected to activate T cell-mediated killing and reduce survival of cells (25). Besides W > F substitutions during tryptophan depletion, Y > F and F > Y substitutions were also observed during tyrosine and phenylalanine depletion, respectively (25). Although many amino acid substitutions may result in dysfunctional proteins (Supplementary Figure S6), we observed beneficial cellular effects from I > V substitutions in healthy primary fibroblasts. PolyPhen-2 HumVar analyses and substitutions in conserved regions support benign effects and tolerance to I > V as opposed to W > F substitutions (Figure 6A and B) (26). ARS recognize amino acids primarily based on size and physiochemical properties (27). When predicting the effect of an amino acid substitution on protein function as benign based on >50% substitutions with a low probability of damage score according to PolyPhen2 HumVar analyses (Figure 6A), specific substitutions of the essential amino acids isoleucine (I > L/V), lysine (K > R), methionine (M > A/I/L/T/V), threonine (T > A/S/V) and valine (V > I/L) may support translational and cellular functions. Of these, I > V, K > R, M > I/L, T > A/S and V > I substitutions are indeed common in conserved regions of proteins (> mean + 1 SD; Figure 6B) (28). Although still requiring confirmation, for these amino acids, tRNA misacylation may help to maintain cellular functions in response to (local) deficiency of essential amino acids and this mechanism may represent a method to preserve translation in response to (local) amino acid deficiencies. This is further supported by recent studies by the group of O'Donoghue showing that mistranslation at different codons is tolerated under normal conditions (29) and may help to preserve normal growth (30).

Nevertheless, there are also examples of detrimental effects of mistranslation caused by mutations in ARS enzymes that disrupt the editing function. Ala > Ser mistranslation causes cerebellar Purkinje cell loss and ataxia in mice as result of accumulation of misfolded proteins (31). Our computational analyses show that A > S mutations are benign in 57% of cases. In that light, while the I > V substitutions may benefit the cell in the short term, long-term effects are still unknown. Introduction of an editing-deficient VARS1—that shares its highly conserved CP1 editing domain with IARS1—into mammalian cells disrupted cell morphology and increased polyubiquitination (32). However, translational fidelity comes at the cost of translational progress, which can also be deleterious. For example, a single mutation (Lys20Arg) in the small ribosomal subunit RPS23 causes hyper accuracy of translation by reduction of stop-codon readthrough. Yeast, worms and flies with this mutation have significantly reduced heat-shock induced ER stress and have 9–23% increased lifespans at the cost of severe developmental delay and growth deficiency. This mutation is conserved in archaea. In organisms living in less harsh environments than archaea, translational flexibility supporting rapid growth and reproduction were evolutionary more important (33).

We previously showed that cognate amino acid supplementation was beneficial in recessive ARS disease (5). Our results do not support supplementing alternative amino acids (e.g. valine) to rescue the (I)ARS1 disease phenotype. However, we noticed that intracellular aspartic acid concentrations were significantly decreased in IARS1 patient fibroblasts and further decrease upon isoleucine starvation. This may be the result of decreased mitochondrial respiration required to produce electron acceptors necessary for de novo synthesis of aspartic acid (34). In fact, supplementation of aspartic acid has been shown to improve respiration defects, causing an increased proliferation rate (35). It would be interesting to assess the effects of aspartic acid supplementation in IARS1 deficiency and other ARS deficiencies with mitochondrial dysfunction.

With our experiments, we further elucidate the disease mechanism of IARS1 deficiency (Figure 5D). Autosomal recessive mutations in IARS1 result in decreased aminoacylation of $tRNA^{Ile}$ (1,5) (Figure 2), which leads to an increase in uncharged $tRNA^{Ile}$. Uncharged tRNAs can bind to GCN2 kinase and thereby slow down translation (36). When an isoleucine codon is not matched by a charged $tRNA^{Ile}$ despite translational slowdown, for example in case of repetitive isoleucine codons or (local) isoleucine deprivation, translation is terminated (Figure 4B). Abnormal truncated peptides trigger the unfolded protein response (Figure 5C), thereby generating cellular stress and further reducing cellular proliferation (Figure 4C). Effects of insufficiency of isoleucine aminoacylation of $tRNA^{Ile}$ in IARS1 deficiency may further be aggravated by additional failure of valine misacylation of $tRNA^{Ile}$ as a compensatory response to isoleucine deprivation. This underlines the importance of specific isoleucine supplementation to support tRNA aminoacylation, protein translation and cellular function in patients with IARS1 deficiency (5).

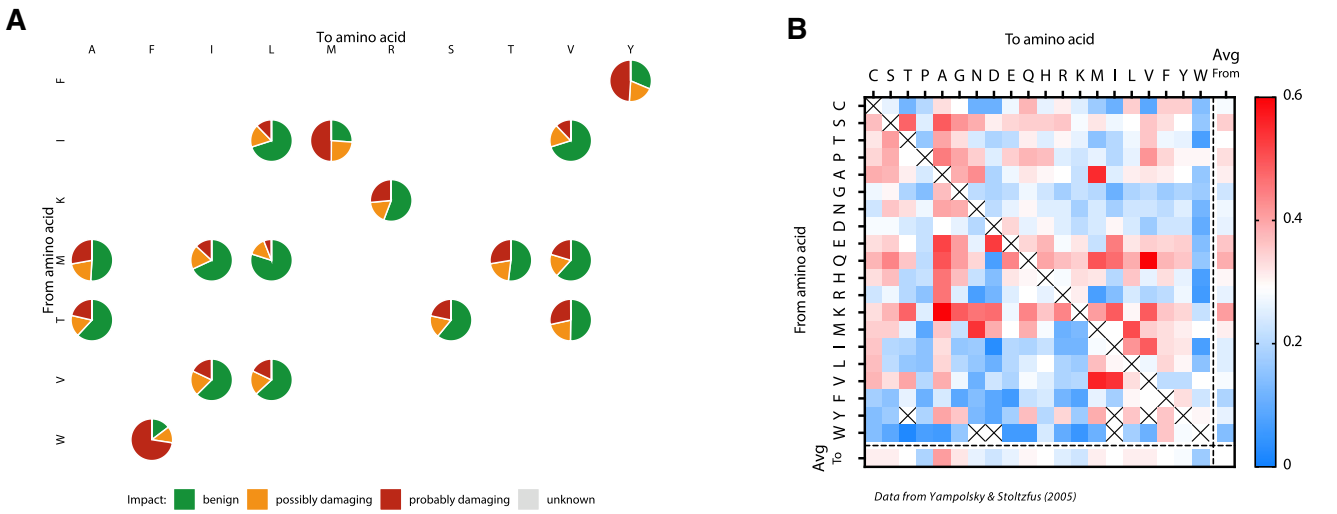

Figure 6. Frequencies of amino acid substitutions in conserved protein and prediction of effect on protein function. (**A**) PolyPhen-2 HumVar analysis probability of damage scores of all plausible substitutions for essential amino acids. PolyPhen-2 predicts the impact of an amino acid substitution on protein structure and function. Scores from 0.0 to 0.15 are predicted benign, 0.15–0.85 possibly damaging and 0.85–1.0 probably damaging (20). (**B**) Heatmap of amino acid exchangeability as calculated by Yampolsky & Stoltzfus (28).

In conclusion, we show that isoleucine to valine substitutions by IARS1 help to prevent translational termination and maintain cellular function in human primary cells during isoleucine deprivation. We suggest that in response to (local) amino acid deficiencies, amino acid substitutions may temporarily help preserve translational speed at the cost of translational fidelity.

Data availability

Mass spectrometry proteomics data have been deposited to the ProteomeXchange Consortium via the PRIDE partner repository (http://www.ebi.ac.uk/pride with the dataset identifier PXD033426). Raw read counts of RNA data are available as supplementary material. Fastq files are not available as we do not have explicit permission to share traceable patient data. All biological materials used in this manuscript are primary patient materials from our hospital. Access is therefore restricted but may be arranged upon reasonable request.

Supplementary data

Supplementary Data are available at NAR Online.

Acknowledgements

We would like to thank Marvin Tanenbaum for fruitful early discussions on this project and for suggesting the concept of a dual fluorescent translation reporter, and Michal Mokry for his assistance with mRNA sequencing and processing of the raw data. We further would like to thank Fabricio Loayza-Puch and Michael VanInsberghe for their help with elucidating the IARS1 disease mechanism. We acknowledge Ehsan Ghayoor Karimiani for supplying patient cells. Lastly, we acknowledge Eline Kormelink for her assistance with various laboratory experiments.

Author contributions: G.K., I.F.S., H.R.V. and S.A.F. conceptualized the study. All experiments with cultures were performed by G.K., I.F.S. and E.F.I., and analyses, statistics and visualization were performed by G.K. and I.F.S. T.A.H. helped design the dual-fluorescent stalling reporter. H.R. performed the IARS1 protein analyses. M.I.M., D.E.C.S. and G.S. performed aminoacylation measurements. E.F.I. and J.J.M.J. measured intracellular amino acid concentrations. E.G.K. provided additional patient cells. H.R.V. and R.M.V.E performed the mass spectrometry, and H.R.V. and P.S. performed the mass spectrometry data analyses and visualization. G.K., I.F.S., E.E.S.N., H.R.V. and S.A.F. drafted and edited the manuscript. The funding sources did not influence any aspect of this study and publishing of this study.

Funding

Stichting Metakids (to S.F.); Netherlands Organization for Health Research and Development (ZonMw) [116002008 and 90714537 to S.F.]; Hereditary Metabolic Diseases in the Dutch Language Area (ESNLT) (to G.K.); Nederlandse Organisatie voor Wetenschappelijk Onderzoek (NWO) [184.034.019 to H.R.V.]. Open access publication was provided by ZonMw.

Conflict of interest statement

None declared.

References

1. Fuchs,S.A., Schene,I.F., Kok,G., Jansen,J.M., Nikkels,P.G.J., van Gassen,K.L.I., Terheggen-Lagro,S.W.J., van der Crabben,S.N., Hoeks,S.E., Niers,L.E.M., *et al.* (2019) Aminoacyl-tRNA synthetase deficiencies: in search of common themes. *Genet. Med.*, **21**, 319–330.
2. Griffin,L.B., Sakaguchi,R., McGuigan,D., Gonzalez,M.A., Searby,C., Züchner,S., Hou,Y.-M. and Antonellis,A. (2014) Impaired function is a common feature of neuropathy-associated glycyl-tRNA synthetase mutations. *Hum. Mutat.*, **35**, 1363–1371.
3. Zuko,A., Mallik,M., Thompson,R., Spaulding,E.L., Wienand,A.R., Been,M., Tadenev,A.L.D., van Bakel,N., Sijlmans,C., Santos,L.A., *et al.* (2021) tRNA overexpression rescues peripheral neuropathy

caused by mutations in tRNA synthetase. *Science*, **373**, 1161–1166.
4. Mendonsa,S., von Kuegelgen,N., Bujanic,L. and Chekulaeva,M. (2021) Charcot–Marie–Tooth mutation in glycyl-tRNA synthetase stalls ribosomes in a pre-accommodation state and activates integrated stress response. *Nucleic Acids Res.*, **49**, 10007–10017.
5. Kok,G., Tseng,L., Schene,I.F., Dijsselhof,M.E., Salomons,G., Mendes,M.I., Smith,D.E.C., Wiedemann,A., Canton,M., Feillet,F., *et al.* (2021) Treatment of ARS deficiencies with specific amino acids. *Genet. Med.*, **23**, 2202–2207.
6. Lenz,D., Stahl,M., Seidl,E., Schöndorf,D., Brennenstuhl,H., Gesenhues,F., Heinzmann,T., Longerich,T., Mendes,M.I., Prokisch,H., *et al.* (2020) Rescue of respiratory failure in pulmonary alveolar proteinosis due to pathogenic *MARS1* variants. *Pediatr. Pulmonol.*, **55**, 3057–3066.
7. Hadchouel,A., Drummond,D., Pontoizeau,C., Aoust,L., Hurtado Nedelec,M.-M., El Benna,J., Gachelin,E., Perisson,C., Vigier,C., Schiff,M., *et al.* (2022) Methionine supplementation for multi-organ dysfunction in MetRS-related pulmonary alveolar proteinosis. *Eur. Respir. J.*, **59**, 2101554.
8. Mordret,E., Dahan,O., Asraf,O., Rak,R., Yehonadav,A., Barnabas,G.D., Cox,J., Geiger,T., Lindner,A.B. and Pilpel,Y. (2019) Systematic detection of amino acid substitutions in proteomes reveals mechanistic basis of ribosome errors and selection for translation fidelity. *Mol. Cell*, **75**, 427–441.
9. Rubio Gomez,M.A. and Ibba,M. (2020) Aminoacyl-tRNA synthetases. *RNA*, **26**, 910–936.
10. Mohler,K. and Ibba,M. (2017) Translational fidelity and mistranslation in the cellular response to stress. *Nat. Microbiol.*, **2**, 17117.
11. Loftfield,R.B. and Vanderjagt,D. (1972) The frequency of errors in protein biosynthesis. *Biochem. J.*, **128**, 1353–1356.
12. Hale,S.P., Auld,D.S., Schmidt,E. and Schimmel,P. (1997) Discrete determinants in transfer RNA for editing and aminoacylation. *Science*, **276**, 1250–1252.
13. Schmidt,J.A., Rinaldi,S., Scalbert,A., Ferrari,P., Achaintre,D., Gunter,M.J., Appleby,P.N., Key,T.J. and Travis,R.C. (2016) Plasma concentrations and intakes of amino acids in male meat-eaters, fish-eaters, vegetarians and vegans: a cross-sectional analysis in the EPIC-Oxford cohort. *Eur. J. Clin. Nutr.*, **70**, 306–312.
14. Pezo,V., Metzgar,D., Hendrickson,T.L., Waas,W.F., Hazebrouck,S., Döring,V., Marlière,P., Schimmel,P. and De Crécy-Lagard,V. (2004) Artificially ambiguous genetic code confers growth yield advantage. *Proc. Natl Acad. Sci.*, **101**, 8593–8597.
15. Juszkiewicz,S. and Hegde,R.S. (2017) Initiation of quality control during poly (A) translation requires site-specific ribosome ubiquitination. *Mol. Cell*, **65**, 743–750.
16. Prinsen,H.C.M.T., Schiebergen-Bronkhorst,B.G.M., Roeleveld,M.W., Jans,J.J.M., De Sain-van Der Velden,M.G.M., Visser,G., Van Hasselt,P.M. and Verhoeven-Duif,N.M. (2016) Rapid quantification of underivatized amino acids in plasma by hydrophilic interaction liquid chromatography (HILIC) coupled with tandem mass-spectrometry. *J. Inherit. Metab. Dis.*, **39**, 651–660.
17. Baydoun,A.R., Emery,P.W., Pearson,J.D. and Mann,G.E. (1990) Substrate-dependent regulation of intracellular amino acid concentrations in cultured bovine aortic endothelial cells. *Biochem. Biophys. Res. Commun.*, **173**, 940–948.
18. Dall'Asta,V., Rossi,P.A., Bussolati,O. and Gazzola,G.C. (1994) Regulatory volume decrease of cultured human fibroblasts involves changes in intracellular amino-acid pool. *Biochim. Biophys. Acta BBA - Mol. Cell Res.*, **1220**, 139–145.
19. Bergström,J., Fürst,P., Norée,L.O. and Vinnars,E. (1974) Intracellular free amino acid concentration in human muscle tissue. *J. Appl. Physiol.*, **36**, 693–697.
20. Adzhubei,I., Jordan,D.M. and Sunyaev,S.R. (2013) Predicting functional effect of human missense mutations using PolyPhen-2. *Curr. Protoc. Hum. Genet.*, **76**, 7.20.1–7.20-41.
21. Love,M.I., Huber,W. and Anders,S. (2014) Moderated estimation of fold change and dispersion for RNA-seq data with DESeq2. *Genome Biol.*, **15**, 550.
22. Xie,Z., Bailey,A., Kuleshov,M.V., Clarke,D.J.B., Evangelista,J.E., Jenkins,S.L., Lachmann,A., Wojciechowicz,M.L., Kropiwnicki,E., Jagodnik,K.M., *et al.* (2021) Gene set knowledge discovery with Enrichr. *Curr. Protoc.*, **1**, e90.
23. Schmidt,E. and Schimmel,P. (1994) Mutational isolation of a sieve for editing in a transfer RNA synthetase. *Science*, **264**, 265–267.
24. Zivkovic,I., Ivkovic,K., Cvetesic,N., Marsavelski,A. and Gruic-Sovulj,I. (2022) Negative catalysis by the editing domain of class I aminoacyl-tRNA synthetases. *Nucleic Acids Res.*, **50**, 4029–4041.
25. Pataskar,A., Champagne,J., Nagel,R., Kenski,J., Laos,M., Michaux,J., Pak,H.S., Bleijerveld,O.B., Mordente,K., Navarro,J.M., *et al.* (2022) Tryptophan depletion results in tryptophan-to-phenylalanine substitutants. *Nature*, **603**, 721–727.
26. Henikoff,S. and Henikoff,J.G. (1992) Amino acid substitution matrices from protein blocks. *Proc. Natl Acad. Sci.*, **89**, 10915–10919.
27. Kaiser,F., Krautwurst,S., Salentin,S., Haupt,V.J., Leberecht,C., Bittrich,S., Labudde,D. and Schroeder,M. (2020) The structural basis of the genetic code: amino acid recognition by aminoacyl-tRNA synthetases. *Sci. Rep.*, **10**, 12647.
28. Yampolsky,L.Y. and Stoltzfus,A. (2005) The exchangeability of amino acids in proteins. *Genetics*, **170**, 1459–1472.
29. Hasan,F., Lant,J.T. and O'Donoghue,P. (2023) Perseverance of protein homeostasis despite mistranslation of glycine codons with alanine. *Philos. Trans. R. Soc. B Biol. Sci.*, **378**, 20220029.
30. Davey-Young,J., Hasan,F., Tennakoon,R., Rozik,P., Moore,H., Hall,P., Cozma,E., Genereaux,J., Hoffman,K.S., Chan,P.P., *et al.* (2024) Mistranslating the genetic code with leucine in yeast and mammalian cells. *RNA Biol.*, **21**, 1–23.
31. Lee,J.W., Beebe,K., Nangle,L.A., Jang,J., Longo-Guess,C.M., Cook,S.A., Davisson,M.T., Sundberg,J.P., Schimmel,P. and Ackerman,S.L. (2006) Editing-defective tRNA synthetase causes protein misfolding and neurodegeneration. *Nature*, **443**, 50–55.
32. Nangle,L.A., Motta,C.M. and Schimmel,P. (2006) Global effects of mistranslation from an editing defect in mammalian cells. *Chem. Biol.*, **13**, 1091–1100.
33. Martinez-Miguel,V.E., Lujan,C., Espie–Caullet,T., Martinez-Martinez,D., Moore,S., Backes,C., Gonzalez,S., Galimov,E.R., Brown,A.E.X., Halic,M., *et al.* (2021) Increased fidelity of protein synthesis extends lifespan. *Cell Metab.*, **33**, 2288–2300.
34. Sullivan,L.B., Gui,D.Y., Hosios,A.M., Bush,L.N., Freinkman,E. and Vander Heiden,M.G. (2015) Supporting aspartate biosynthesis is an essential function of respiration in proliferating cells. *Cell*, **162**, 552–563.
35. Birsoy,K., Wang,T., Chen,W.W., Freinkman,E., Abu-Remaileh,M. and Sabatini,D.M. (2015) An essential role of the mitochondrial electron transport chain in cell proliferation is to enable aspartate synthesis. *Cell*, **162**, 540–551.
36. Pavlova,N.N., King,B., Josselsohn,R.H., Violante,S., Macera,V.L., Vardhana,S.A., Cross,J.R. and Thompson,C.B. (2020) Translation in amino-acid-poor environments is limited by tRNAGln charging. *eLife*, **9**, e62307.

Received: September 15, 2022. **Revised:** November 8, 2024. **Editorial Decision:** November 11, 2024. **Accepted:** November 13, 2024